Molecular Physics, 2014
Vol. 112, Nos. 5–6, 575–582, http://dx.doi.org/10.1080/00268976.2013.832429

INVITED ARTICLE

$S_0 \rightarrow S_3$ transition in recombination products of photodissociated dihalomethanes

Ignacio Fdez. Galván[a,*], Hong-Yan Xiao[b], Isabelle Navizet[c,d], Ya-Jun Liu[d,*] and Roland Lindh[a]

[a]*Department of Chemistry – Ångström, The Theoretical Chemistry Programme, Uppsala University, PO Box 518, SE-751 20 Uppsala, Sweden;* [b]*Key Laboratory of Photochemical Conversion and Optoelectronic Materials, Technical Institute of Physics and Chemistry, Chinese Academy of Sciences, Beijing 100190, China;* [c]*Laboratoire de Modelisation et Simulation Multi Echelle, University Paris-Est, MSME UMR 8208 CNRS, 5 bd. Descartes, 77454 Marne-la-Vallée, France;* [d]*College of Chemistry, Beijing Normal University, Beijing 100875, China*

(*Received 19 June 2013; accepted 31 July 2013*)

Species of the form CH_2X–Y (X, Y = Br, I) have been proposed and identified as recombination products of the photodissociation of the parent dihalomethanes. Second-order complete active space perturbation theory (CASPT2) calculations of the vertical absorption energies considerably overestimate the experimental transient absorption band maxima, while the computationally cheaper time-dependent density functional theory (TD-DFT) method yields results with a reasonable agreement. In this work, we try to find the reason for this unexpected performance difference. In an initial study of the I_2 molecule, we establish that CASPT2 is capable of providing quantitatively accurate results and that the TD-DFT values are only valid at first sight, but are qualitatively flawed. In the CASPT2 calculations for the CH_2X–Y molecules, we include relativistic corrections, spin–orbit coupling, vibrational and thermal effects, and the solvent polarisation. Unfortunately, the results do not improve appreciably compared to the experimental measurements. We conclude that the good agreement of TD-DFT results is very likely fortuitous in this case as well, and that further theoretical and experimental investigations are probably needed to resolve the current discrepancy between CASPT2 and experiments.

Keywords: dihalomethanes; transient absorption; spin–orbit coupling; rovibronic transitions

1. Introduction

The photodissociation of dihalomethanes containing bromine and/or iodine has been experimentally and theoretically studied because of their importance in atmospheric chemistry, their use in organic chemistry, and the possibility of considering them as model systems for understanding the fundamental photochemical reactions in laser-induced dissociations and the subsequent recombination process.

Experimental studies on the photodissociation reactions in solutions and in cold solid matrices have detected short-lived photoproducts with characteristic absorption bands in the 300–800 nm region, which have been identified as the recombination isomers CH_2X–Y (X, Y = Br, I) [1–6]. Apparently, the parent CH_2X Y molecule suffers a cleavage of the C–Y bond, resulting in the CH_2X and Y initial fragments. In the gas phase these fragments separate, but within the cage provided by the solvent or solid environment they can recombine to form the CH_2X–Y isomer to some measurable extent.

Theoretical calculations have helped establishing the identity of the CH_2X–Y species and the photolysis pathways of the parent dihalomethanes [2–4,7–9]. It is, however, significant that calculations with a multiconfigurational method such as multistate second-order complete active space perturbation theory (MS-CASPT2)/CASPT2, which has often been shown to be highly reliable, predict absorption maxima that are at least 0.5 eV too high compared to the experimental results. Meanwhile, the computationally cheaper time-dependent density functional theory (TD-DFT) with Becke's three-parameter Lee-Yang-Parr (B3LYP) hybrid functional method yields values in reasonable agreement with the experiments. Other features of the CH_2X–Y species, like vibrational frequencies or a lower energy absorption band, are correctly reproduced by CASPT2.

In this work, we address the discrepancy between CASPT2 and experiments in the location of the absorption maxima at around 400 nm (3.1 eV). We study the four CH_2X–Y species mentioned, focusing on the corresponding electronic transition ($S_0 \rightarrow S_3$). In the CASPT2 calculations, we include relativistic corrections and spin–orbit coupling, and we analyse how the temperature, vibrational levels and solvent influence can affect the absorption maximum. With this, we try to identify the reason for the disappointing CASPT2 results and whether the TD-DFT ones can be relied on or they must be considered accidental.

2. Method and details

The ground-state, S_0, geometries of CH_2Br–Br, CH_2Br–I, CH_2I–Br and CH_2I–I were optimised at the CASPT2

*Corresponding authors. Email: ignacio.fernandez@teokem.uu.se; yajun.liu@bnu.edu.cn

[10] level with a state averaging (SA) of six roots in the complete active space self-consistent field (CASSCF) reference. Potential energy curves were also obtained along the interhalogen distance, r(X–Y), coordinate: for fixed X–Y distances between 2.5 and 6.0 Å the rest of the coordinates were optimised on the ground-state surface. Vertical excitation energies (T_V) and oscillator strength (f) values were evaluated for a number of electronic states (six singlets and five triplets, 6s+5t) obtained with the MS-CASPT2 method [11]. Spin–orbit coupled (SOC) states were also obtained by applying the complete active space state interaction (CASSI) treatment on top of the MS-CASPT2 results [12], in conjunction with the atomic mean-field integral [13] approximation. Solvent effects, when included, were introduced with the polarisable continuum model (PCM) method [14] or its conductor version (C-PCM) [15], by using non-equilibrium conditions on the excited state.

The active space used was 12 electrons in eight orbitals (12e,8o), including the p orbitals of the halogens and the s and p orbitals of C, except those involved in C–H bonds. The C[He], Br[Ar] and I[Kr] cores were left uncorrelated at the (MS-)CASPT2 level. The basis set used in all calculations was ANO-RCC [16], with triple-ζ contraction on the valence shell and polarisation functions (ANO-RCC-VTZP). Scalar relativistic effects were included in all CASPT2 calculations through the second-order Douglas–Kroll–Hess transformation, and the default ionisation energy−electron affinity (IP−EA) shift of 0.25 E_h [17] was applied to the zeroth-order Hamiltonian. No symmetry constraints were applied. All these calculations were performed with the Molcas 7 quantum chemistry software [18].

For benchmarking, some additional calculations were run on the I_2 molecule. In this case, the same methods described above were used, with a full valence (14e,8o) active space, and the states included in the CASSI-SOC calculations were 5s+5t and 10s+10t. For comparison, we also treated the I_2 molecule with spin-unrestricted (TD-)DFT methods, using the B3LYP hybrid functional, and with the basis sets ANO-RCC-VTZP, Sadlej-pVTZ [19] and aug-cc-pVTZ-PP [20]. Scalar relativistic corrections were included in all CASPT2 calculations and some of the DFT calculations; these are indicated with 'DKH2'. All DFT calculations were done with the Gaussian 09 quantum chemistry software [21] and included the first 20 singlet or triplet roots with the TD-DFT treatment.

2.1. *Rovibronic analysis*

In order to include the contribution from the different rovibronic transitions to the final absorption spectra, we computed the ro-vibrational levels on the ground and excited electronic states, as well as their relative population and probability of transition between them. For this task we used the VibRot program included in Molcas. For each potential energy curve (E vs. r) the ro-vibrational Schrödinger equation is solved numerically, and the overlap between the wave functions of the different electronic states can be computed. The transition probability (oscillator strength, f_{ij}) can be obtained by incorporating the r-dependent transition dipole moment, μ_T, between the two electronic states in the overlap calculation:

$$f_{ij} \propto \int \Phi''_i(r)\Phi'_j(r)\mu_T(r)r^2 \, dr, \qquad (1)$$

where Φ''_i and Φ'_j are the i and j normalised ro-vibrational wave functions on the ground and excited electronic states, respectively.

To simulate the absorption spectrum, we assign to each $i \rightarrow j$ transition an intensity proportional to f_{ij} and to the Boltzmann population of the ground-state level i at the desired temperature. A Lorentz-type curve of a given width, centred at the corresponding transition energy and with an area proportional to the intensity, is generated for each transition, and the sum of all these curves is the final simulated spectrum.

Obtaining the potential energy curves for the I_2 molecule is simple, as the r coordinate is trivially the I–I distance. For the CH_2X–Y molecules we had to use a reduced dimension, since the method is only applicable to diatomic molecules. We represented the CH_2X–Y molecules as fictitious Q–Y diatomic molecules, where Q is a pseudo-atom that replaces the CH_2X moiety, with its mass, and located at its centre of mass (quite close to the X atom). The energy curves of CH_2X–Y along the r(X–Y) coordinate were then referred to the Q–Y distance, and we proceeded as described.

Table 1. Equilibrium distance, r_e, and vertical absorption energy, T_V, for the I_2 molecule obtained at different calculation levels.

	r_e (Å)	T_V (eV)
MS(5s+5t)-CASPT2	2.652	2.32
MS(10s+10t)-CASPT2	2.651	2.32
UB3LYP/Sadlej	2.719	2.15
UB3LYP/aug-cc	2.703	2.09
UB3LYP/ANO+DKH2	2.692	2.16
UB3LYP/Sadlej+DKH2	2.563	2.55
Experimental [22–25]	2.666	2.34

3. Results and discussion

3.1. *I_2 molecule*

As an assessment of the quality of the methods used, we performed an initial study of the I_2 molecule. The equilibrium bond length r_e was found by minimisation of the energy, and values thus obtained are given in Table 1. We note first that the CASPT2 results are very close to the accepted

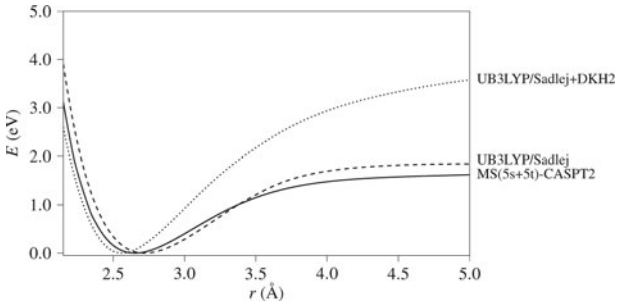

Figure 1. Potential energy curves for the I_2 molecule with three selected methods. Each curve is shifted to have the minimum at 0 eV. MS(10s+10t)-CASPT2 is almost coincident with MS(5s+5t)-CASPT2, and UB3LYP/aug-cc and UB3LYP/ANO+DKH2 are very similar to UB3LYP/Sadlej.

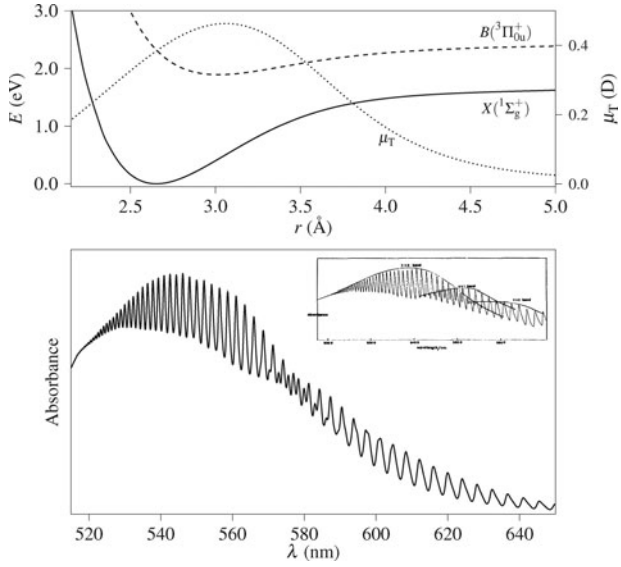

Figure 2. Top panel: potential energy curves of the ground and excited states of I_2 (left-hand axis), and transition dipole moment, μ_T (right-hand axis), calculated at the SOC-MS(5s+5t)-CASPT2 level. Bottom panel: simulated absorption spectrum at 300 K from the data above. Inset: experimental spectrum, reprinted with permission from Ref. [25] (Copyright (1987) [American Chemical Society]).

experimental value (2.666 Å), while DFT calculations show larger deviations. Non-relativistic calculations overestimate the bond distance by 0.04–0.05 Å, and the use of a relativistic basis set (ANO-RCC-VTZP) together with the scalar correction makes it somewhat better. However, including the correction with a non-relativistic basis set (Sadlej+DKH2) results in an underestimation of 0.1 Å.

A scan of the potential energy curves was done for bond lengths between 2 and 5 Å, and some of the curves are shown in Figure 1. Most DFT curves are very similar to each other and, considering the shift of the minimum distance, are also very similar to the CASPT2 curves around the minimum, the main difference being the dissociation energy, which is ∼0.3 eV larger with DFT. The most striking difference is the UB3LYP/Sadlej+DKH2 curve, which once again shows that one should not use relativistic corrections with a non-relativistic basis set.

We also computed the vertical absorption energies, T_V, at equilibrium geometries, for the transition with the highest oscillator strength in the region corresponding to the $X(^1\Sigma_g^+) \rightarrow B(^3\Pi_{0u}^+)$ transition of I_2. The values are also displayed in Table 1. Again, we find a very good agreement of CASPT2 results with the experiment. TD-DFT results are underestimated by 0.15–0.20 eV, but adding the DKH2 correction with a non-relativistic basis set increases the T_V value by 0.4 eV, making it overestimated instead.

The computed T_V values, in the SOC-CASPT2 calculations, correspond to the transition to the sixth excited state, which is almost a pure triplet, while the ground state has an ∼2% triplet character. The excited-state curve has a minimum at around 3.0 Å (see Figure 2), comparable to the literature value of 3.024 Å [24]. In contrast, the T_V values reported for TD-DFT calculations correspond to the $S_0 \rightarrow S_1$ transition, involving only singlet states; the closest triplet states are at ∼1.5 and ∼3.1 eV above the ground-state minimum, much farther from the experimental absorption maximum. In the SOC-CASPT2 calculations, there is a predominantly singlet state at around 2.45 eV which should probably be compared to the S_1 state in the TD-DFT results.

From the CASPT2 calculations we could obtain smooth potential energy curves for both the ground state (X) and the excited state (B), which allowed us to compute the vibrational levels in both states and the vibrational structure of the corresponding absorption band, as described above. The simulated absorption spectrum, displayed in Figure 2, is very similar to the experimental one [25], the envelopes corresponding to $v'' = 0$, 1 and even 2 can be distinguished, and the maximum absorption occurs at around 545 nm (2.27 eV), which slightly deviates the T_V result in Table 1 from the experimental reported value of 529 nm (2.34 eV). In addition, we also calculated the vibrationally averaged expectation value for the bond length r, which is 2.666 Å at 300 K and 2.675 Å at 450 K (compare the latter with the experimental 2.681 Å [26]).

The TD-DFT curves for the excited states, however, have some continuity issues (cusps) around 3.3–3.6 Å and are not appropriate for a vibrational analysis.

Taking all these results together, it seems that SOC-MS-CASPT2/ANO-RCC-VTZP is capable of giving results in qualitative and quantitative agreement with the experiment. The shape of the potential energy curves, position of the minima, vertical absorption energy, nature of the electronic states and vibrational structure of the absorption band all match very closely the available experimental data. This therefore supports the validity of the method for studying the CH_2X–Y (X, Y = Br, I) systems, which would conceivably require a similar level of theory. On the other hand, the different DFT results show a number of issues:

Table 2. Interhalogen bond lengths (in Å) and vertical excitation energies to the S_3 state (in eV) for the CH_2X–Y molecules.

	CH_2Br–Br	CH_2I–Br	CH_2Br–I	CH_2I–I
r(X–Y)				
CASPT2[a]	2.625	2.734	2.830	2.950
T_V				
CASPT2[a]	4.06	4.01	3.86	3.85
TD-B3LYP	3.32[b]	3.46[c]	2.94[c]	2.92[e]
Experimental	∼3.44[b]	∼3.10–3.44[c]	2.80[d]	∼3.22[e]

Notes: [a]SOC-MS(6s+5t)-CASPT2/SA(6)-CAS(12,8)PT2/ANO-RCC-VTZP. [b]Ref. [3]. [c]Ref. [4]. [d]Ref. [5]. [e]Ref. [2].

although the equilibrium bond length is approximately correct, there are discontinuity problems at longer distances in the potential energy curves; the computed vertical absorption energies are not too far from the experimental values, but the excited state is identified as a singlet and no triplet candidate is found nearby, which leads to the conclusion that the apparently good result is in this case only fortuitous.

3.2. *CH_2X–Y systems*

We carried out for the CH_2X–Y (X, Y = Br, I) systems a similar study to that performed for I_2. A more detailed report on the geometry and electronic structure of these systems has already been published in previous works [7–9]. In this paper, we concentrate on analysing the transition assigned to the experimental band found at 370–450 nm, due to the significant difference between the computed and experimental values.

The geometry of each molecule was optimised at the CASPT2/ANO-RCC-VTZP level, and a scan of the potential energy surface was done by varying the X–Y distance and optimising the other degrees of freedom. The optimised X–Y distances are shown in Table 2. At each point of these scans, single-point calculations were done with SOC-MS(6s+5t)-CASPT2, and the vertical transition energies were computed to the excited state with largest oscillator strength in the region of 3–4 eV, which in all cases was a state with the main contribution from the fourth singlet, and we will refer to it as S_3 even if it has some mixing with other spin-free states. The T_V values obtained at the optimised geometries are given in Table 2. We note that some results differ from those published earlier at a similar computational level by 0.1–0.2 eV, which is due to the different value of the IP−EA shift, which is 0.25 E_h in this work and by default in Molcas versions since 6.4, while previous versions had no such shift.

In general, the perturbed zero-order wave functions of both the ground and excited states are described with the same two electron configurations, one of closed-shell type and the other of diradical type. The ground state can be described as composed of ∼60% of the closed shell and ∼25% of the diradical, while the excited S_3 state is ∼20% closed shell and ∼50% diradical. The $S_0 \rightarrow S_3$ transition thus corresponds to a redistribution of these configurations and the overall electron density decreases near the C and X atoms, while it increases on the Y atom. It must be noted that the above characterisation of the states is only valid in terms of the average orbitals obtained by the SA-CASSCF procedure, and the description would change if a different set of orbitals, such as state-specific natural orbitals, were used.

The first observation from Table 2 is that the X–Y bond distances are rather long (compare with the Br_2, IBr and I_2 bond distances: 2.281, 2.469 and 2.666 Å, respectively [24]). The I–I distance in CH_2I–I has been determined experimentally through picosecond X-ray diffraction at 3.02 ± 0.02 Å [6]. In comparison, the present value is somewhat lower, while the B3LYP/TZVP result reported in Ref. [2] is much closer, 3.042 Å. However, it must be considered that the experiment measures the average distance and not the equilibrium distance, and, when vibrational averaging at 300 K is included (see below), the predicted CASPT2 distance is 2.982 Å, and a similar increase would be expected for B3LYP values. Thus, a comparable performance of these methods is found to what was described above for I_2, where CASPT2 slightly underestimates and B3LYP overestimates the bond length.

Another observation from Table 2 is that all the computed absorption energies are very similar to each other, with those for species where Y = I being ∼0.2 eV lower than for Y = Br. This is a result of the electron structure being rather similar in all these species, and supports including all of them in a single study. However, the main motive for this work is the fact that in all species the computed transition energies are 0.4–1.0 eV higher than the experimental transient absorption bands attributed to them. As shown in previous works [7–9], in all the CH_2X–Y systems the active S_3 state is the 13th SOC state at the equilibrium geometry, and the oscillator strength for the $S_0 \rightarrow S_3$ transition is of the order of 0.6. The immediately lower states are 1.0–1.5 eV below S_3 and their oscillator strengths are at least two orders of magnitude weaker. Thus, it does not seem likely that the experimental absorption around 3 eV be due to any other state than the S_3 state studied here; in fact, a lower energy band has been found in argon matrices which agrees quite well with the strongest transitions below the S_3 state [1].

Surprisingly, the TD-DFT calculations reported by other authors give results in very good agreement with the experiment, except maybe for the CH_2I–I species. This is striking due to the above-mentioned partial diradical character of the ground state, which would be expected to deteriorate the quality of DFT methods. Besides, these TD-DFT calculations did not include relativistic effects, which may

be important for the present systems, and this could be one reason for the poorer performance of CH_2I–I.

In spite of the apparent good performance of TD-DFT, these results should be taken with caution. We note that there is a significant uncertainty in the experimental maximum absorption of CH_2I–Br and that the value for CH_2Br–I was obtained in acetonitrile as solvent, while the other experiments were done in cyclohexane. Comparison with the CH_2I–I absorption (3.22 eV in cyclohexane [2]; 3.14 eV in acetonitrile [27]) would give ∼2.90 eV for CH_2Br–I in cyclohexane. Nevertheless, TD-DFT estimations are much closer to experiment than CASPT2 ones. Given the usually very good performance of CASPT2 and the frequent problems of TD-DFT, as demonstrated in the I_2 case above, we believe that the good TD-DFT agreement is accidental and that there is some factor unaccounted for in the calculations or in the interpretation of the experiments that causes the rather large and systematic discrepancy with CASPT2. In the following, we try to include as many of these factors as possible, hoping to bring the CASPT2 results closer to experimental values.

Active space and basis set. The active space used for the CH_2X–Y calculations is somewhat reduced compared to that used for I_2. We tested how this fact could affect the results. First, we applied a smaller active space to the I_2 calculations, excluding the s orbitals, which leaves (10e, 6o). The equilibrium bond distance was not affected, and the T_V value was 0.06 eV higher than with the larger active space. We then performed some additional single-point calculations on CH_2X–Y systems, with an extended active space which includes the full valence shell, that is, (20e,14o). Similarly to the I_2 case, the vertical transition energies are reduced by ∼0.05 eV or less with the larger active space. To test the influence of the basis set, we did some single-point calculations on CH_2X–Y species with a larger basis set, by using a quadruple-ζ contraction of the ANO-RCC set (ANO-RCC-VQZP). In this case, the T_V values are only reduced by ∼0.02 eV. These results indicate that the basis set and the active space chosen for the main CH_2X–Y calculations do only introduce minor errors in the transition energies and the conclusions are therefore not affected.

Spin–orbit coupling effect on the geometry. In the above results, the transition energies were calculated by including the SOC through the CASSI treatment of the MS-CASPT2 wave functions, but the geometries were optimised at the single-state, spin-free CASPT2 level. Although the SOC effect on the geometry is expected to be minor, it could still have a significant effect on the transition energies. The S_3 state is bonded, but it has the minimum at longer X–Y distances and it is quite repulsive in the S_0 minimum region. For example, in CH_2Br–Br (see Figure 3) a lengthening of the Br–Br distance by 0.05 Å would reduce T_V by 0.15 eV,

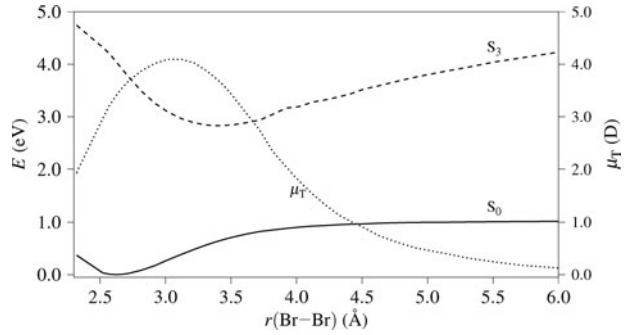

Figure 3. SA(6)-CAS(12,8)PT2/ANO-RCC-VTZP potential energy curves of the two electronic states studied for CH_2Br–Br. The transition dipole moment, μ_T, is also represented as a dotted line.

and the experimental value would be obtained at r(Br–Br) ≃ 2.8 Å. On the contrary, the S_0 curve is quite flat, as can be deduced from the vibrational frequency (see below), and at 2.8 Å the ground-state energy is only about 8 kJ mol^{-1} above the minimum.

We computed the SOC-MS(6s+5t)-CASPT2 energies for all the points along the SA(6)-CAS(12,8)PT2/ANO-RCC-VTZP curves. For the new potential energy curves thus obtained along the r(X–Y) coordinate, we calculated the interpolated minimum on the S_0 state and the T_V value to the S_3 state. The results, displayed in Table 3, showed only a very slight shift in the minimum position, lower than 0.02 Å in all cases, smaller and to shorter distances for Y = Br and somewhat larger and to longer distances for Y = I. The interpolated T_V values do not differ much from those of Table 2, only ± 0.01 eV, except for CH_2Br–I where the change is −0.04 eV. It therefore does not look like the SOC effect on the geometries is a significant factor in the discrepancy between CASPT2 and experimental absorption energies.

Table 3. Equilibrium interhalogen bond lengths (in Å) and vertical excitation energies to the S_3 state (in eV) for the CH_2X–Y molecules including SOC and solvent effects. All T_V values are computed at the SOC-MS(6s+5t)-CASPT2 level (with PCM if in solution); the differences are in the energies used for locating the minimum of the potential energy curves (see text).

	CH_2Br–Br	CH_2I–Br	CH_2Br–I	CH_2I–I
r(X–Y)				
CASPT2	2.625	2.734	2.830	2.950
SOC-MS-CASPT2	2.624	2.729	2.847	2.957
PCM-SOC-MS-CASPT2	2.608	2.654	2.846	2.848
T_V				
CASPT2	4.06	4.01	3.86	3.85
SOC-MS-CASPT2	4.06	4.02	3.82	3.84
PCM-SOC-MS-CASPT2	4.12	4.08	3.89	3.86

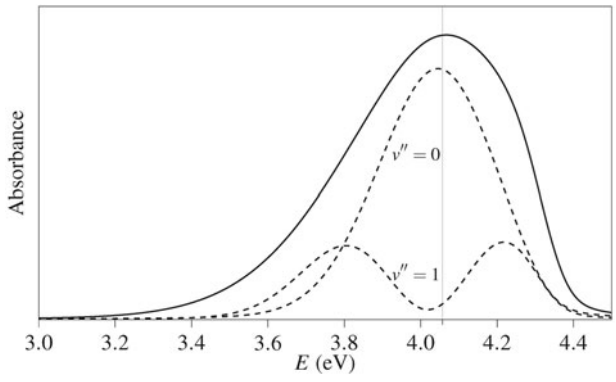

Figure 4. Simulated absorption spectrum (full line) of CH_2Br–Br at 300 K from SOC-MS(6s+5t)-CASPT2//SA(6)-CAS(12,8)PT2/ANO-RCC-VTZP potential energy curves. The vertical line marks the computed T_V value at the equilibrium geometry. The dashed lines show the contribution of two different S_0 vibrational levels (the full line contains further terms).

Vibration and temperature. As discussed above, the X–Y bond in the CH_2X–Y molecules is relatively long and weak; the experimental frequencies assigned to its stretching are in the range 130–180 cm^{-1} [2–4]. This means that vibrational levels are close to each other, higher levels can be populated at room temperature and the vibrational motion can shift the absorption maximum from the value at the ground-state equilibrium distance. It has already been mentioned that vibrational averaging elongates the effective X–Y bond in CH_2I–I: the effect is computed to be 0.010–0.045 Å in all four species. This alone could explain part of the discrepancy, as longer distances would result in lower T_V (Figure 3). However, the expected effect must be confirmed with an analysis of the vibrational structure of the $S_0 \rightarrow S_3$ band.

To perform this analysis, we computed the vibrational levels in both the S_0 and S_3 states and the simulated absorption spectrum, as detailed in Section 2. As a result, we find that although levels up to $v'' = 7$ are populated with at least 1% of the $v'' = 0$ population, the maximum of the absorption band hardly changes from the computed T_V at the S_0 minimum (differences of 0.01 eV or less). This happens because the lower-energy contribution from one end of the vibration is compensated by the higher-energy contribution from the other end. An example is shown in Figure 4.

Thus, although the lengthening of the average X–Y bond is appreciable at room temperature, the predicted shift in the absorption maximum is negligible, at least with the simple diatomic model we used.

Solvent effect. So far, we have been comparing the calculations performed on isolated molecules with the experimental results, which have been measured in solution. In most of the experiments, the solvent is cyclohexane, and such a non-polar solvent is not expected to induce dramatic changes in the electronic states of the solute. In addition, the absorption band does not seem to be extremely sensitive to solvent polarity (0.08 eV redshift from cyclohexane to acetonitrile for CH_2I–I [2,27]). Nevertheless, since the computed T_V can be significantly affected by small changes in the molecular structure, we analysed the effect that the inclusion of the solvent effect has on the results.

As with SOC effects on the geometry, the solvent effect was included by performing single-point calculations with the PCM model on the SA(6)-CAS(12,8)PT2/ANO-RCC-VTZP optimised structures along the r(X–Y) coordinate. We used the solvent parameters appropriate for the experiment on each molecule, i.e. cyclohexane for all except acetonitrile for CH_2Br–I (in the latter case, the C-PCM solvation model was employed). The resulting PCM-SOC-MS(6s+5t)-CASPT2 curves were interpolated to get the X–Y distance and T_V value at the minimum.

In general, the solvent makes the X–Y distances around 0.00–0.02 Å shorter for X = Br and 0.08–0.09 Å shorter for X = I, which in turn increases the T_V values in ~0.07 eV (0.02 eV for CH_2Br–I) (see Table 3). The shape of the curves and the nature of the S_0 and S_3 states are not altered by the solvent, so the vibrational analysis, as in the gas phase, does not give an appreciable shift in the absorption maximum from the T_V value.

Hence, we find that the bulk solvent effect is not responsible for the CASPT2–experiment disagreement, and including it only enhances the disagreement.

4. Conclusion

We have carried out a unified study of the $S_0 \rightarrow S_3$ absorption in CH_2X–Y (X, Y = Br, I) molecules, which have been proposed as recombination products found in the photodissociation of dihalomethanes CH_2X Y. Previous calculations with a high-level multiconfigurational method, such as CASPT2, showed a significant discrepancy between the computed vertical absorption energy and the experimental transient absorption maximum. In this work, we have tried to address this issue and refine the computational results, by including additional effects like spin–orbit coupling, the solvent effect or the temperature-dependent population of vibrational levels.

A benchmark calculation on the I_2 molecule showed that the level we have used is capable of providing very good results in qualitative and quantitative agreement with the experimental data available. This gives us some confidence to apply the same method to the CH_2X–Y molecules, which should pose a similar 'difficulty'.

In spite of our efforts, we always found absorption energies much too high compared to the experimental results.

The extent of the overestimation, 0.4–1.0 eV, is unusual for a state-of-the-art CASPT2 calculation in a system of this size, and we could not identify the source of this discrepancy in the calculations.

Rather surprisingly, TD-DFT calculations seem to give transition energy values much closer to the experiments. As shown with I_2, it is possible for TD-DFT calculations to yield an apparently 'correct' result that, upon closer examination, raises serious doubts about its validity. As Zheng and Phillips mentioned [2], the errors associated with the TD-DFT method they used can be of about the same size as found with CASPT2 for these systems. Besides, the nature of the CH_2X–Y species, where the ground state is a mixture of closed-shell and diradical structures, makes it especially unlikely for DFT to succeed in describing the electronic structure, while CASPT2 fails. For these reasons, we believe that the good agreement of the reported TD-DFT results with the experimental values must be considered an accident, albeit a fortunate one.

However, although a part of the evidence supporting the existence of the CH_2X–Y forms is based on the DFT calculations, we do not believe there is enough reason to discard these species as recombination products. CASPT2 and DFT calculations still agree fairly well with the vibrational frequencies obtained from resonance Raman spectra [2,7,9], and DFT frequency calculations are generally much more reliable than excitation energies. Moreover, a weaker absorption band found at lower energies is also very well reproduced with CASPT2 calculations [1,7,8], and there is strong evidence supporting that the ∼3.0–3.5 eV band here studied belongs to the same species.

The calculations performed for this work have not allowed us to reproduce the experimental absorption maxima, even though we have used some of the best quality methods available. We do not believe this is due to a shortcoming of the theoretical methods employed. Nonetheless, one could still think of further effects not considered here which might explain the difference. (1) We assumed the interhalogen X–Y distance as the main coordinate affecting the T_V values; the CH_2 degrees of freedom could have an effect that would need to be investigated. (2) Although the solvent effect on T_V is expected to be minor, our calculations used standard PCM parameters, while the X–Y bond is rather unusual; it might be that the PCM parameters used are not appropriate for describing the solvation in the CH_2X–Y systems. (3) In relation to this, the PCM method can only include inespecific or bulk solvent effects, and maybe specific solute–solvent associations are important, or there could be associations with other species or impurities present in the experiment responsible for the discrepancy. (4) Experiments in cold matrices tend to give higher energies for the band maximum [1]; this could be an indication that dynamical effects due to the solvent and the increased temperature may play a significant role in lowering the transition energy.

Acknowledgements

Roland Lindh would like to thank the Swedish Research Council (VR) for financial support.

Funding

This research is supported by the National Nature Science Foundation of China [grant number 21003143], [grant number 20873010], [grant number 20720102038]; the Major State Basic Research Development Programs [grant number 2007CB815206]; SRF for ROCS, SEM. The research at KAIST is supported by funds from the National Research Foundation [grant number 2009-0053704], [grant number R111-2007-012-03001-0]; the KISTI Supercomputing Center.

References

[1] G. Maier, H.P. Reisenauer, J. Hu, L.J. Schaad, and B.A. Hess, Jr, J. Am. Chem. Soc. **112**, 5117 (1990).
[2] X. Zheng and D.L. Phillips, J. Phys. Chem. A **104**, 6880 (2000).
[3] X. Zheng, W.M. Kwok, and D.L. Phillips, J. Phys. Chem. A **104**, 10464 (2000).
[4] X. Zheng and D.L. Phillips, J. Chem. Phys. **113**, 3194 (2000).
[5] A.N. Tarnovsky, M. Wall, M. Gustafsson, N. Lascoux, V. Sundström, and E. Åkesson, J. Phys. Chem. A **106**, 5999 (2002).
[6] J. Davidsson, J. Poulsen, M. Cammarata, P. Georgiou, R. Wouts, G. Katona, F. Jacobson, A. Plech, M. Wulff, G. Nyman, and R. Neutze, Phys. Rev. Lett. **94**, 245503 (2005).
[7] Y.-J. Liu, D. Ajitha, J.W. Krogh, A.N. Tarnovsky, and R. Lindh, ChemPhysChem **7**, 955 (2006).
[8] Y.-J. Liu, L. De Vico, R. Lindh, and W.-H. Fang, ChemPhysChem **8**, 890 (2007).
[9] Y.-J. Liu, H.-Y. Xiao, M. Sun, and W.-H. Fang, J. Comput. Chem. **29**, 2513 (2008).
[10] K. Andersson, P.-Å. Malmqvist, and B.O. Roos, J. Chem. Phys. **96**, 1218 (1992).
[11] J. Finley, P.-Å. Malmqvist, B.O. Roos, and L. Serrano-Andrés, Chem. Phys. Lett. **288**, 299 (1998).
[12] B.O. Roos and P.-Å. Malmqvist, Phys. Chem. Chem. Phys. **6**, 2919 (2004).
[13] C.M. Marian and U. Wahlgren, Chem. Phys. Lett. **251**, 357 (1996).
[14] S. Miertuš, E. Scrocco, and J. Tomasi, Chem. Phys. **55**, 117 (1981).
[15] M. Cossi, N. Rega, G. Scalmani, and V. Barone, J. Comput. Chem. **24**, 669 (2003).
[16] B.O. Roos, R. Lindh, P.-Å. Malmqvist, V. Veryazov, and P.-O. Widmark, J. Phys. Chem. A **108**, 2851 (2004).
[17] G. Ghigo, B.O. Roos, and P.-Å. Malmqvist, Chem. Phys. Lett. **396**, 142 (2004).
[18] G. Karlström, R. Lindh, P.-Å. Malmqvist, B.O. Roos, U. Ryde, V. Veryazov, P.-O. Widmark, M. Cossi, B. Schimmelpfennig, P. Neogrády, and L. Seijo, Comput. Mater. Sci. **28**, 222 (2003).
[19] A. Sadlej, J.,Theor. Chim. Acta **81**, 339 (1992).
[20] K.A. Peterson, D. Figgen, E. Goll, H. Stoll, and M. Dolg, J. Chem. Phys. **119**, 11113 (2003).
[21] M.J. Frisch, G.W. Trucks, H.B. Schlegel, G.E. Scuseria, M.A. Robb, J.R. Cheeseman, G. Scalmani, V. Barone, B. Mennucci, G.A. Petersson, H. Nakatsuji, M. Caricato, X. Li, H.P. Hratchian, A.F. Izmaylov, J. Bloino, G. Zheng, J.L. Sonnenberg, M. Hada, M. Ehara, K. Toyota, R.

Fukuda, J. Hasegawa, M. Ishida, T. Nakajima, Y. Honda, O. Kitao, H. Nakai, T. Vreven, J.A. Montgomery, Jr., J.E. Peralta, F. Ogliaro, M. Bearpark, J.J. Heyd, E. Brothers, K.N. Kudin, V.N. Staroverov, R. Kobayashi, J. Normand, K. Raghavachari, A. Rendell, J.C. Burant, S.S. Iyengar, J. Tomasi, M. Cossi, N. Rega, J.M. Millam, M. Klene, J.E. Knox, J.B. Cross, V. Bakken, C. Adamo, J. Jaramillo, R. Gomperts, R.E. Stratmann, O. Yazyev, A.J. Austin, R. Cammi, C. Pomelli, J.W. Ochterski, R.L. Martin, K. Morokuma, V.G. Zakrzewski, G.A. Voth, P. Salvador, J.J. Dannenberg, S. Dapprich, A.D. Daniels, Ö. Farkas, J.B. Foresman, J.V. Ortiz, J. Cioslowski, and D.J. Fox. *Gaussian 09 (Revision C.01)* (Gaussian, Inc., Wallingford, CT, 2009).

[22] R.D. Verma, J. Chem. Phys. **32**, 738 (1960).

[23] R. D'alterio, R. Mattson, and R. Harris, J. Chem. Educ. **51**, 282 (1974).

[24] K.P. Huber and G. Herzberg, in *NIST Chemistry WebBook*, edited by P.J. Linstrom and W.G. Mallard (NIST Standard Reference Database Number 69; National Institute of Standards and Technology, Gaithersburg, MD, 2013).

[25] R.B. Snadden, J. Chem. Educ. **64**, 919 (1987).

[26] U. Buontempo, A. Di Cicco, A. Filipponi, M. Nardone, and P. Postorino, J. Chem. Phys. **107**, 5720 (1997).

[27] A.N. Tarnovsky, J.-L. Álvarez, A.P. Yartsev, V. Sundström, and E. Åkesson, Chem. Phys. Lett. **312**, 121 (1999).